JTTEE5 17:473–477
DOI: 10.1007/s11666-008-9201-5

Peer Reviewed

Preparation of TiO_2 Nanopowders by Plasma Spray and Characterizations

Lajun Feng, Dapeng Xu, and Ali Lei

(Submitted December 6, 2007; in revised form January 21, 2008)

TiO_2 powders with the range of 10-60 nm were prepared successfully by plasma spray in the self-developed plasma spray equipment. The prepared nanopowders were characterized by transmission electron microscopy, X-ray diffraction, and X-ray photoelectron spectroscopy. The results showed that the prepared TiO_2 nanopowders were the mixture of anatase phase and rutile phase, the main phase was anatase. There were O, Ti, and C elements in powders; Ti element still existed in tetravalent. The photocatalytic degradation of methyl orange indicated that all methyl orange (20 mg/L) can be degraded fully when the addition of prepared TiO_2 nanopowders and illumination time were 1 g/L and 150 min, respectively.

Keywords plasma spray, TEM, TiO_2 photocatalyst, XPS, XRD

1. Introduction

Since nanoparticles in the size range of 1-100 nm have unique surface effect, small-scale effect, quantum effect, mechanical properties, optical properties, thermal properties, and chemical properties, the investigation of nanomaterials has been becoming a hot topic (Ref 1-3). TiO_2 nanopowders have extensive application in photocatalyzed field because of characteristics such as innocuity, strong oxidizability, fine stability, high light-transfer characteristic, etc. (Ref 4).

At present, most of the preparing methods are sol-gel route (Ref 5), immersion method (Ref 6, 7), magnetron sputtering method (Ref 8), etc. Plasma spray is a method to prepare wear-resistant coating (Ref 9), in which molten metal powders and high-melting point powder are sprayed on the substrate, and the use of plasma spray is widespread recently (Ref 10-15). As thermal plasma has high temperature, high enthalpy, high thermal gradient, etc. (Ref 16), the uniform nanopowders can be prepared when the atomized liquid transfer through plasma torch and react quickly in the plasma.

Owing to simple technical process, fast reaction, and easy industrialization, it is significant to investigate plasma spray for nanophase materials. In this study, the solution of titanium tetra-tert-butoxide and ethanol absolute were used as spraying material for TiO_2 nanopowders. The morphology, phases, crystallite size, and element quantivalency were characterized by transmission electron microscopy (TEM), X-ray diffraction (XRD), and X-ray photoelectron spectroscopy (XPS). The efficiency of photocatalytic degradation of methyl orange with prepared TiO_2 nanopowders under different irradiation time was discussed as well. The investigation provides a new method for preparing nanopowders and has a theoretical significance for the investigation and application of TiO_2 nanopowders.

Lajun Feng, Dapeng Xu, and **Ali Lei**, School of Materials Science and Engineering, Xi'an University of Technology, Xi'an 710048, P.R. China. Contact e-mail: fenglajun@xaut.edu.cn.

2. Experimental

2.1 Materials

Titanium tetra-tert-butoxide with chemical reagent grade, ethanol absolute (≥99.7%) with analytical reagent grade, methyl orange with chemical reagent grade, and de-ionized water were used in the investigation.

2.2 Preparation of TiO_2 Nanopowders

Liquid plasma spray system developed by Xi'an University of Technology was adopted as the spraying equipment, which is consisted of general GP-80 plasma spray equipment equipped with liquid feeding-in system (Ref 17). Sketch map of the liquid plasma spray is shown in Fig. 1.

Spraying liquid was a mixture of titanium tetra-tert-butoxide and ethanol absolute with the volume fraction of 1:1. Firstly, the spray liquid was atomized into very fine drippings and then the drippings were entered into plasma region by using self-made atomizing nozzle with two-fluid pattern (as shown in Fig. 2) as transfusion equipment. The atomized drippings have the pyrolytic cracking chemical reaction in plasma to produce minute solid particles. The particles were sent into electrostatic precipitator about 40 cm from self-made atomizing nozzle by plasma gas flow and then collected (Ref 17). The key of preparing TiO_2 nanopowders by liquid plasma spray was to control the

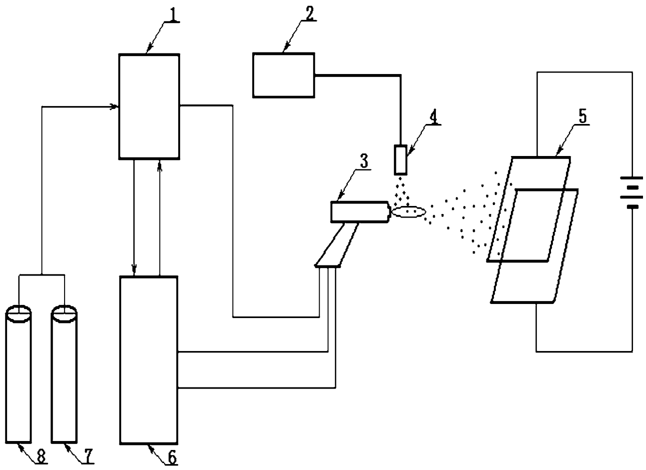

Fig. 1 Sketch map of the liquid plasma spray. 1, control console; 2, liquid infusion; 3, plasma spraying gun; 4, atomizing nozzle; 5, electrostatic precipitator; 6, power supply; 7, argon gas; 8, hydrogen gas

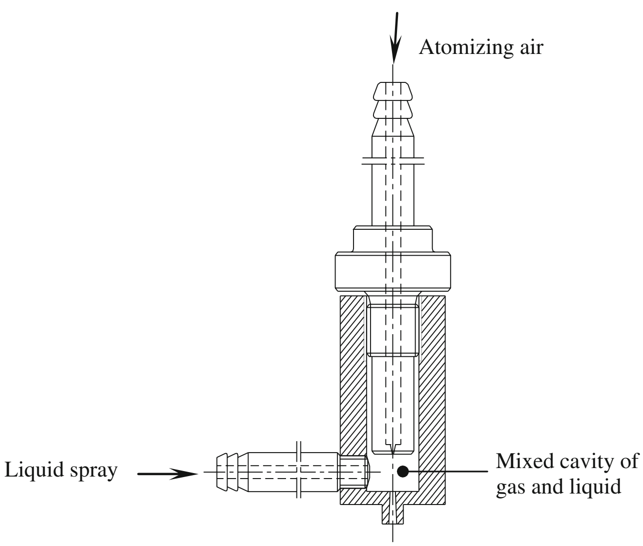

Fig. 2 The atomizing nozzle with two-fluid pattern

sizes of atomization drippings and the intensity of plasma torch. The diameters of drippings were mainly controlled by the diameter of atomizing nozzle and the pressure of atomizing atmosphere, and the temperature of plasma torch can be rectified by the pressure of hydrogen gas, current, and voltage. The optimized technological parameters of plasma spray are given in Table 1.

2.3 Characterization of TiO_2 Nanopowders

The morphology and distribution of crystallite size of powders prepared were characterized by JEM-3010 TEM. The crystal structure of powders was analyzed by XRD-7000S X-ray diffractometer. X-ray source and the scanning rate of diffraction angle 2θ are CuKα (λ = 0.15418 nm) and 10°/min, respectively. The mass fraction of anatase phase and rutile phase in powders is counted in terms of the relative intensity of maximum anatase phase peak (101) and maximum rutile phase peak (110); the formula is as follows:

Table 1 Optimized technological parameters of plasma spray

Parameters	Value
Argon gas pressure, MPa	0.85
Hydrogen gas pressure, MPa	0.12
Atomization gas (O_2) pressure, MPa	0.05
Liquid feedstock, flow/mL min^{-1}	1.17
Current, A	600
Power, kW	33
Diameter of delivering liquid, hole/mm	1.5
Diameter of delivering gas, hole/mm	0.2

$$\omega_A = \frac{I_A}{I_A + 1.265 I_R} 100\% \quad \text{(Eq 1)}$$

where ω_A is the content of anatase phase in powders, I_A is the intensity of maximum anatase phase peak (101), I_R is the intensity of maximum rutile phase peak (110), and the content of rutile phase is $1 - \omega_A$. Scherrer formula (Ref 18) was used to determine average particle size of powders:

$$D = K\lambda / B \cos\theta \quad \text{(Eq 2)}$$

where D is diameter of grain, K is constant, which is usually given 0.89, λ is wavelength of X-ray, B is full width of half maxima (FWHM), and θ is Bragg diffraction angle.

The composition and properties of the products were studied using XPS. The XPS spectra were obtained by Axis Ultra, Kratos (UK), using monochromatic Al Kα radiation (150 W, 15 kV, 1486.6 eV). The vacuum in the spectrometer was 10-9 Torr. Binding energies were calibrated relative to the C1s peak (284.8 eV) from hydrocarbons adsorbed on the surface of the samples.

Photocatalytic performances of the samples were tested by the degradation ratio of methyl orange water solution illuminated by ultraviolet lights. The solution with 20 mg/L concentration was prepared by 100 mL de-ionized water and 2 mg methyl orange ($C_{14}H_{14}N_3NaO_3S$) in 500 mL beaker, and then 0.1 g TiO_2 nanopowders was added to confect a solution with 1 g/L. The mixture was shaked by supersonic vibration for some time to form suspension system. The photocatalytic degradation experiment was firstly conducted under the illumination of ultraviolet lights (2 × 20 W) and electric stirring, then filtrating, and measuring absorbency numerical value with spectrophotometer after the illumination for a certain time. Since the absorbency numerical value at maximal absorptive wavelength 471 nm has a linear relationship with its concentration, the degradation ratio of samples can be obtained in terms of the variation of samples' absorbency numerical value, and then the degradation ratio of TiO_2 photocatalyst was characterized. The formula is as follows:

$$P = (A_0 - A_t)/A_0 \times 100\% \quad \text{(Eq 3)}$$

where P is the degradation ratio of methyl orange samples, A_0 is the absorbency numerical value of samples before photocatalytic degradation, and A_t is the absorbency numerical value of samples after photocatalytic degradation for t time.

3. Results and Discussion

3.1 TEM Analysis

Figure 3 shows the TEM micrograph of TiO_2 nanopowders prepared by plasma spray. It can be seen that the prepared nanopowders' size was in the range of 10-60 nm and the prepared powders had globular shape or approximate globular shape. Nanopowder particle size depends on the atomized drop size, controlled by the atomization pressure and way of injection (axially or transversely). These liquid drops are obtained from various processes such as deformation/break up, precipitation, evaporation, and pyrolysis (Ref 19). The critical radius of crystal nucleus is related to the degree of supersaturation (Ref 20). The flame flow of plasma had two extreme conditions—the high temperature and the rapid cooling [In the solution plasma various size of drops are injected inside the plasma plume and go through the above mentioned path. The time of flight is short (in microseconds) and does not allow the particles to grow.], which make the system to have high supersaturation and form a large number of nucleus. Because the time of nucleus growth is shortened by the splat cooling, the powders prepared with nanometer scale can be obtained.

3.2 XRD Analysis

The XRD pattern of TiO_2 nanopowders prepared by plasma spray is shown in Fig. 4. It can be seen that the angle of the main diffraction peak is 25.3, which is corresponded with diffraction plane of anatase phase TiO_2 (101).

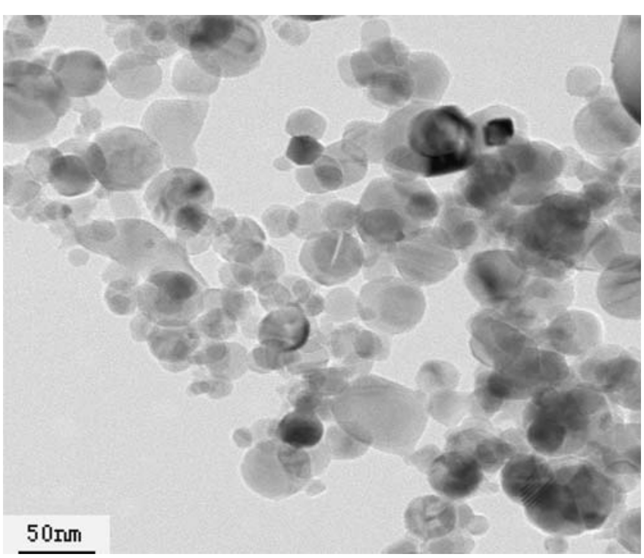

Fig. 3 TEM micrograph of TiO_2 nanopowders prepared by plasma spray

The phase fraction and crystallite size of TiO_2 nanopowders were calculated according to Formula 1 and 2. The results are given in Table 2. As expected, the formed sample was the mixed crystals of anatase phase and rutile phase, and the main phase was anatase.

It also can be seen from Table 2 that the crystallite size of anatase phase was smaller than that of rutile phase. Because quasi-stable anatase phase has higher free energy in spraying process, it prefers to nucleate in flame flow and inborn crystal grains occur to phase transformation when heated. Owing to larger surface energy on the surface of crystal grain, rutile phase will nucleate preferentially on the surface of anatase phase crystal grain and block the growth of anatase phase crystal grain so that the particle size of rutile phase is larger than that of anatase phase.

3.3 XPS Analysis

Figure 5-7 show XPS survey spectra, XPS spectra of the O 1s region, and XPS spectra of the Ti 2p region of TiO_2 nanopowders prepared by plasma spray, respectively.

As shown in Fig. 5, there were O, Ti, and C elements in the prepared powders. C element mainly comes from polluted XPS experimental installation and the others were the undecomposed precursor of organic substances.

It can be seen from Fig. 6 that O 1s region was decompounded into three parts including Ti–O bond from TiO_2, surface hydroxy group and adsorbed H_2O, and the main constituent was corresponded to Ti–O bond.

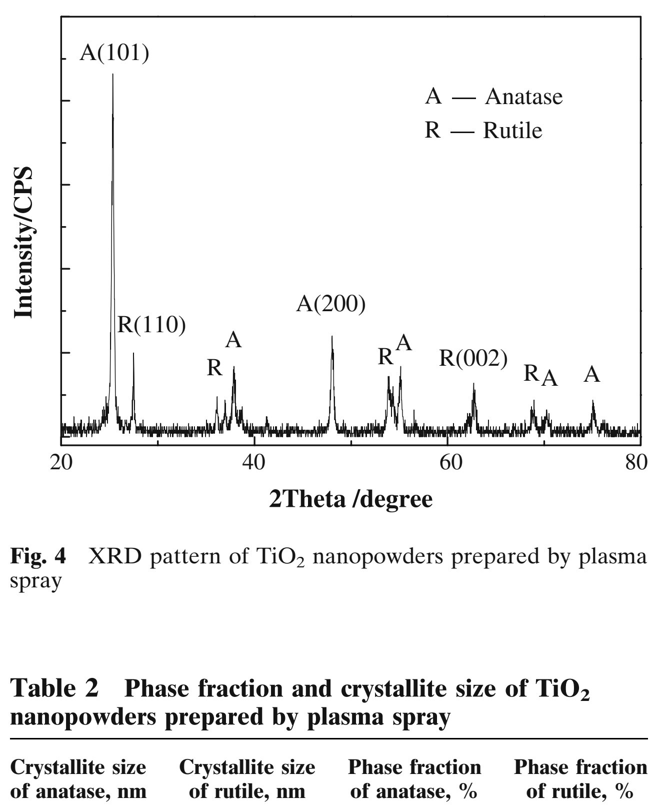

Fig. 4 XRD pattern of TiO_2 nanopowders prepared by plasma spray

Table 2 Phase fraction and crystallite size of TiO_2 nanopowders prepared by plasma spray

Crystallite size of anatase, nm	Crystallite size of rutile, nm	Phase fraction of anatase, %	Phase fraction of rutile, %
29.40	53.27	80.62	19.38

Peer Reviewed

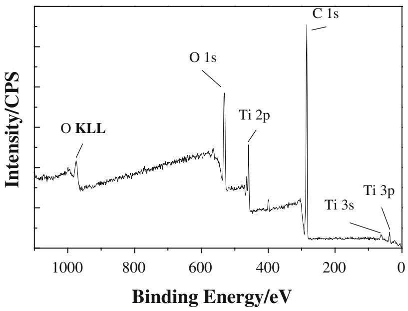

Fig. 5 XPS survey spectra of TiO_2 nanopowders prepared by plasma spray

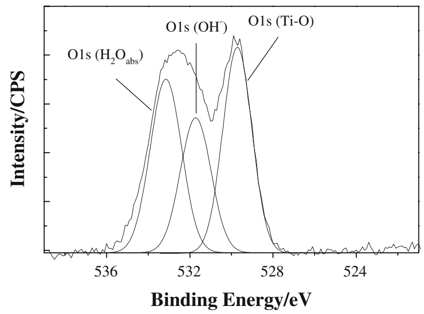

Fig. 6 XPS spectra of the O 1s region of TiO_2 nanopowders prepared by plasma spray

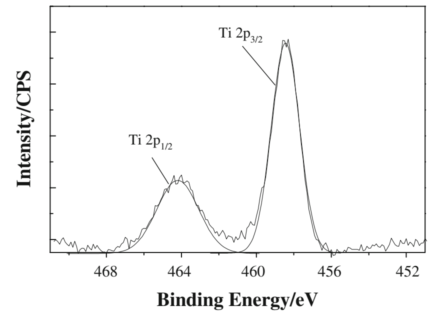

Fig. 7 XPS spectra of the Ti 2p region of TiO_2 nanopowders prepared by plasma spray

Nanophase materials absorb H_2O easily because of their high specific area; meanwhile, H_2O can also react with TiO_2 to form Ti–OH. This chemical reaction was shown as follows:

$$H_2O + Ti{-}O{-}Ti \rightarrow 2Ti{-}OH.$$

During the photocatalytic process, the surface hydroxy group may become hydroxy-free radical and almost all the organic pollutants are oxygenized and degraded into inorganic small molecules such as CO_2 and H_2O due to the function of hydroxy-free radical with strong oxidizing property created from the system.

Figure 7 shows that the Ti 2p region was composed of $2p_{3/2}$ peak and $2p_{1/2}$ peak. The area ratio of A(Ti $2p_{1/2}$) and A(Ti $2p_{3/2}$) is approximately 0.4 and the difference of binding energy is about 5.7 eV. The binding energies of $2p_{3/2}$ peak and $2p_{1/2}$ peak are 458.4 ± 0.1 eV and 464.1 ± 0.1 eV, respectively, which are well in accordance with that of Ti(+4) given by the standard manual (Ref 21), and it is also indicated that all Ti in powders existed in the form of TiO_2. Zhang (Ref 22) and Zhang (Ref 23) found that Ti existed in the form of oxides with low valence such as Ti(+3) and Ti(+2); however, only Ti(+4) is found in the present investigation. It is thought that the atomizing gas in preparing powder is oxygen with strong oxidizing property and oxygen can also participate in reaction besides atomization, so Ti can be fully oxidized into Ti(+4).

3.4 Results of Photocatalysis

Figure 8 shows the change of methyl orange concentration with radiation time using TiO_2 nanopowders prepared by plasma spray.

It can be seen that the degradation rate of methyl orange increased with radiation time. When the radiation time was 150 min, all methyl orange was degraded. The main reason is that the prepared TiO_2 is in nanograde scale and nano-TiO_2 is nanosemiconductor particle, which has quantum size effect, thus leading to widen the energy gap of conduction band and valence band; the electric potential of conduction band becomes more negative and the electric potential of valence band becomes more positive (Ref 24). It suggests that the nanosemiconductor particle has stronger reductive and oxidative ability,

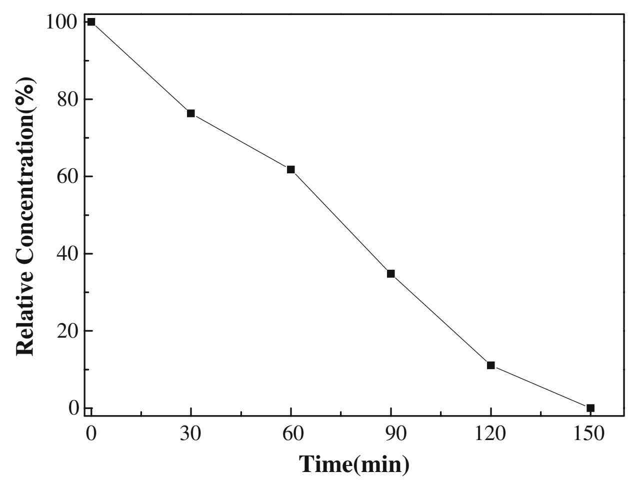

Fig. 8 Change of methyl orange concentration with radiation time using TiO_2 nanopowders prepared by plasma spray

thereby increasing the photocatalytic activity. Also, the smaller the particle diameter is, the shorter is the route from the inside of particle to the surface of particle for the photoelectron and cavity diffusion and the less probability of recombination is, so increases the efficiency of photocatalytic activity.

4. Conclusion

1. TiO_2 nanopowders were prepared by plasma spray using the solution of titanium tetra-tert-butoxide and ethanol absolute as spray feed; the range of the powder size was 10-60 nm and they had globular shape or approximate globular shape.
2. The prepared powders were the mixture of anatase phase and rutile phase, and the anatase was the main phase. The crystallite size of anatase phase was smaller than that of rutile phase.
3. There were O, Ti, and C elements in the powders. O 1s region was decompounded into three parts and Ti 2p region was composed of $2p_{3/2}$ peak and $2p_{1/2}$ peak. Ti element was still tetravalent.

4. The degradation rate of methyl orange increases with radiation time and all methyl orange (20 mg/L) can be degraded fully when the addition of prepared TiO_2 nanopowders and illumination time were 1 g/L and 150 min, respectively.

References

1. J.W. Xue, Tribology and Lubricant Technology, 1st ed., Weapon Industry Press, Beijing, 1992, p 1-5
2. J.B. Yao and J.X. Dong, A Tribocatalysis Reaction in Boundary Lubrication—An Antiwear Synergism Between Borates and Copper Oleate, *Lubr. Eng.*, 1995, **51**(3), p 231-233
3. J.B. Yao, J.X. Dong, and R.G. Xiong, Antiwear Synergism of Borates and Copper Oleate, *Lubr. Eng.*, 1994, **50**(9), p 695-698
4. D.A. Tryk, A. Fujishma, and K. Honda, Recent Topics in Photoelectrochemistry: Achievements and Future Prospects, *Electrochim. Acta*, 2000, **45**(15/16), p 2363-2376
5. P. Bonamali, S. Maheshwar, and N. Gyoichi, Preparation and Characterization of TiO_2/Fe_2O_3 Binary Mixed Oxides and Its Photocatalytic Properties, *Mater. Chem. Phys.*, 1999, **59**, p 254-261
6. J.A. Navio, G. Colon, and M. Trilys, Heterogeneous Photocatalytic Reactions of Nitrite Oxidation and Cr(6+) Reduction on Iron-Doped Titania Prepared by the Wet Impregnation Method, *Appl. Catal. B: Environ.*, 1998, **16**(2), p 187-196
7. O. Teruhisa, T. Fumihiro, and F. Kan, Photocatalytic Oxidation of Water by Visible Light Using Ruthenium-Doped Titanium Dioxide Powder, *J. Photochem. Photobiol. A: Chem.*, 1999, **127**, p 107-110
8. K. Zakrzewska, M. Radecka, and A. Kruk, Noble Metal/Titanium Dioxide Nanocermets for Photoelectrochemical Applications, *Solid State Ionics*, 2003, **157**, p 349-356
9. T. Kanazawa and A. Ohmori, Behavior of Coating Formation on PET Plate by Plasma Spraying and Evaluation of Coating's Photocatalytic Activity, *Surf. Coat. Technol.*, 2005, **197**, p 45-50
10. E.H. Jordan, L. Xie, X. Ma, M. Gell, N.P. Padture, B.M. Cetegen, A. Ozture, J. Roth, T.D. Xiao, and P.E. Bryant, Mechanisms of Ceramic Coating Deposition in Solution-Precursor Plasma Spray, *J. Therm. Spray Technol.*, 2004, **13**(1), p 57-65
11. T. Bhatia, A. Ozturk, L. Xie, E. Jordan, B.M. Cetegen, M. Gell, X. Ma, and N. Padture, Mechanisms of Ceramic Coating Deposition in Solution-Precursor Plasma Spray, *J. Mater. Res.*, 2002, **17**(9), p 2363-2372
12. A. Ozturk and B.M. Cetegen, Experiments on Ceramic Formation from Liquid Precursor Spray Axially Injected into an Oxy-Acetylene Flame, *Acta Mater.*, 2005, **53**, p 5203-5211
13. M. Gell, L. Xie, X. Ma, E.H. Jordan, and N. Padture, Highly Durable Thermal Barrier Coatings made by the Solution Precursor Plasma Spray Process, *Surf. Coat. Technol.*, 2004, **177-178**, p 97-102
14. V. Viswanathan and S. Seal, High Temperature Oxidation Behavior of Solution Precursor Plasma Sprayed Nanoceria Coating on Martensitic Steel Substrate, *J Am. Ceram. Soc.*, 2007, **90**(3), p 870-877
15. B.G. Ravi, S. Sampath, R. Gambino, P.S. Devi, and J.B. Parise, Plasma Spray Synthesis from Precursors: Progress, Issues, and Considerations, *J. Therm. Spray Technol.*, 2006, **15**(4), p 701-707
16. Y. Zeng, J.T. Liu, and W.J. Qian, Photocatalytic Performance of Plasma Sprayed TiO_2-$ZnFe_2O_4$ Coatings, *Acta Metall. Sin.*, 2005, **18**(3), p 363-368
17. L.J. Feng and B. Liu, Plasma Spray Synthesis of TiO_2 Nanoparticle, *China Surf. Eng.*, 2004, **65**, p 11-14 (in Chinese)
18. H.Z. Huang, Nanomaterials Analysis, 1st ed., Chemical Industry Press, Beijing, 2003, p 4-9
19. J. Karthikeyan, C.C. Berndt, J. Tikkanen, S. Reddy, and H. Herman, Plasma Spray Synthesis of Nanomaterial Powders and Deposits, *Mater. Sci. Eng. A.*, 1997, **238**(2), p 275-286
20. K.C. Zhang, Crystals Growth, 1st ed., Science Press, Beijing, 1981, p 3-5
21. J.F. Moulder, W.F. Stickle, and P.E. Sobol, Handbook of X-ray Photoelectron Spectroscopy, 2nd ed., Perkin-Elmer Corporation, Minnesota, 2002, p 58-80
22. W.J. Zhang, Y. Li, and S.L. Zhu, Surface Modification of Film by Iron Doping Using Reactive Magnetron Sputtering, *Chem. Phys. Lett.*, 2003, **373**, p 333-337
23. Q. Zhang, X.J. Li, and F.B. Li, Investigation on Visible-light Activity of WO_x/TiO_2 Photocatalyst, *J. Phys. Chem.*, 2004, **20**(5), p 507-511 (in Chinese)
24. G.J. Yang, C.J. Li, and Y.Y. Wang, Phase Formation of Nano-TiO_2 Particles During Flame Spraying with Liquid Feedstock, *J. Therm. Spray Technol.*, 2005, **14**(4), p 480-486